separations

MDPI

Article

Effective Solid Phase Extraction of Toxic Pyrrolizidine Alkaloids from Honey with Reusable Organosilyl-Sulfonated Halloysite Nanotubes

Tobias Schlappack [1,†], Nina Weidacher [1,†], Christian W. Huck [1], Günther K. Bonn [1,2] and Matthias Rainer [1,*]

[1] Institute of Analytical Chemistry and Radiochemistry, Leopold-Franzens-University Innsbruck, Innrain 80/82, A-6020 Innsbruck, Austria
[2] Austrian Drug Screening Institute–ADSI, Innrain 66a, A-6020 Innsbruck, Austria
* Correspondence: m.rainer@uibk.ac.at; Tel.: +43-512-507-57307
† These authors contributed equally to this work.

Abstract: Pyrrolizidine alkaloids are plant secondary metabolites that have recently attracted attention as toxic contaminants in various foods and feeds as they are often harvested by accident. Furthermore, they prove themselves as hard to analyze due to their wide structural range and low concentration levels. However, even low concentrations show toxic behavior in the form of chronic liver diseases and possible carcinogenicity. Since sample preparation for this compound group is in need of more green and sustainable alternatives, modified halloysite nanotubes present an interesting approach. Based on the successful use of sulfonated halloysite nanotubes as inexpensive, easy-to-produce cation exchangers for solid phase extraction in our last work, this study deals with the further modification of the raw nanotubes and their performance in the solid phase extraction of pyrrolizidine alkaloids. Conducting already published syntheses of two organosilyl-sulfonated halloysite nanotubes, namely HNT-PhSO_3H and HNT-MPTMS-SO_3H, both materials were used as novel materials in solid phase extraction. After the optimization of the extraction protocol, extractions of aqueous pyrrolizidine alkaloid mixtures showed promising results with recoveries ranging from 78.3% to 101.3%. Therefore, spiked honey samples were extracted with an adjusted protocol. The mercaptopropyl-sulfonated halloysite nanotubes revealed satisfying loading efficiencies and recoveries. Validation was then performed, which displayed acceptable performance for the presented method. In addition, reusability studies using HNT-MPTMS-SO_3H for solid phase extraction of an aqueous pyrrolizidine alkaloid mixture demonstrated excellent results over six cycles with no trend of recovery reduction or material depletion. Therefore, organosilyl-sulfonated halloysite nanotubes display a green, efficient and low-cost alternative to polymeric support in solid phase extraction of toxic pyrrolizidine alkaloids from complex honey matrix.

Keywords: halloysite nanotubes; organosilyl-sulfonated halloysite nanotubes; solid phase extraction; pyrrolizidine alkaloids; honey

Citation: Schlappack, T.; Weidacher, N.; Huck, C.W.; Bonn, G.K.; Rainer, M. Effective Solid Phase Extraction of Toxic Pyrrolizidine Alkaloids from Honey with Reusable Organosilyl-Sulfonated Halloysite Nanotubes. *Separations* **2022**, *9*, 270. https://doi.org/10.3390/separations9100270

Academic Editor: Attilio Naccarato

Received: 13 September 2022
Accepted: 20 September 2022
Published: 29 September 2022

1. Introduction

Clays are well known to humanity and have been used in a wide range of applications for a long time. However, as humankind continues to evolve, more possibilities for these compounds arise through different methods for controlling their morphological characteristics [1]. One type of material derived from these natural clays is halloysite. Halloysite nanotubes, also called nanosized tubular halloysite or halloysite nanoclay is the naturally most occurring halloysite [2]. Large deposits were found in Australia, the United States, China, New Zealand, Mexico and Brazil [2,3]. Morphologically, halloysite nanotubes are two-layered aluminosilicates with a hollow, tubular structure, which is formed through the rolling of 15 to 20 aluminosilicate layers, similar to carbon nanotubes [2–6]. The external surface consists of silicone dioxide groups, whereas the inner surface is composed

of aluminum oxide groups [7]. It is a member of the kaolin group and shares chemical similarity with kaolinite [2,8,9]. However, monolayers of water molecules separate the unit layers in halloysites in contrast to the layers in kaolinite. Hydrated forms share a sum formula of $Al_2(OH)_4Si_2O_5 \cdot nH_2O$. Halloysite–(10 Å) presents the hydrated form with n = 2 and one layer of water, whereas halloysite–(7 Å) is the name of the dry mineral with n = 0. The angstrom term defines the d_{001}−value of the respective mineral. A conversion from the hydrated to the dry state can be achieved through a mild temperature and/or vacuum. The dimensions of halloysite nanotubes vary from the submicron scale to several microns in length, 30 to 190 nm external diameter and 10 to 100 nm internal diameter [2,5]. However, the morphology and porosity of these halloysites can strongly vary between origins and are influenced through acidic or basic treatment [10,11]. Furthermore, platy and spheroidal morphologies were also observed next to tubular structures, which is the dominant form. This tubular structure is caused by a mismatch between adjacent silicone dioxide and aluminum oxide layers [7]. In the past decade, these tubes became the main focus of many studies and showed promising characteristics [2]. As they are non-toxic, inexpensive, biocompatible, possess high specific surface areas and show different possibilities for inner-outer surface chemistry, the first applications in polymer filling, catalysis, nanoencapsulation and wastewater treatment have already been reported [1,2,5,8,9,12,13]. All these properties make halloysite nanotubes a strong competitor against expensive carbon nanotubes [9], even though carbon nanotubes are currently still in frequent use [14,15]. In addition, the aluminosilicate structure of halloysites with their external siloxane surface gives the possibility of chemically modifying hydroxyl groups on said surface [2,7,8,16,17]. In addition to this, high natural cation exchange capacities of 30–50 $\times$ 10^{-2} mol kg^{-1} suggests favorable ion exchange properties [3]. This opens the possibility for the use of highly selective, chemically modified halloysite nanotubes to extract compounds of interest. In our last work, we presented a method using one-pot synthesized sulfonated halloysite nanotubes (HNT-SO_3H) for the selective solid phase extraction of toxic pyrrolizidine alkaloids from honey [18]. These pyrrolizidine alkaloids present a hepatotoxic and possible cancerogenic group of compounds with over 660 known, highly diverse structures present in over 6000 plant species [19–24]. As they are often harvested by accident they are a highly important topic for food safety, since regular intake of even small amounts can cause chronic liver diseases [22–29]. Furthermore, the transportation of pollen from pyrrolizidine alkaloid-containing plants through bees can contaminate pollen products such as honey as well [19,30]. Highly sensitive methods are needed, since maximum limits of pyrrolizidine alkaloids in food are in the magnitude of micrograms per kilogram [31]. Therefore, working groups and official institutions use solid phase extraction with reversed phase or cation exchange interactions to enrich the alkaloids and reduce the matrix effect before analysis [18,21,30,32–36]. Especially reversed phase methods show lower selectivity in general and can therefore be problematic in terms of interfering compounds and matrix effects. Hence, we want to expand the possibilities for the selective extraction of pyrrolizidine alkaloids from complex matrices and to further reduce the matrix effect. In this study, we synthesized two organosilyl-sulfonated halloysite nanotubes according to previously published studies to selectively extract toxic pyrrolizidine alkaloids from a honey sample [16,17]. Apart from our previously published work, according to our knowledge there has been no application of modified halloysites as solid phase extraction material so far. However, different modifications on the halloysites could provide even better results in solid phase extractions. Furthermore, in addition to the impressive analytical performance of modified halloysite nanotubes, exploring the applicability of these materials for solid-phase extraction is another important building block in making analytical chemistry more environmentally friendly and sustainable, and further eliminating extraction methods using polymer resins.

2. Experimental

2.1. Materials and Methods

2.1.1. Reagents and Standards

Acetonitrile (for LC-MS; ≥99.95%) and methanol (for LC-MS; ≥99.95%) were obtained from Chemsolute® (Th. Geyer, Renningen, Germany). Dichloromethane (for HPLC, 100%) was ordered from VWR (VWR International, Radnor, USA). Chlorosulfonic acid (purum, >98.0% (T)) and dimethyl sulfoxide (p.a.; ACS: >99.9% (GC)) were bought from Fluka AG (Honeywell International Inc., Morristown, NJ, USA). Thiourea (p.a.) was purchase from Merck (Merck KGaA, Darmstadt, Germany) for the determination of dead time. Ammonium formate (≥95%) and formic acid (ROTIPURAN® ≥98%, p.a., ACS) were purchased from Carl Roth (Carl Roth GmbH + Co. KG, Karlsruhe, Germany). Phyproof® reference substances were purchased from PhytoLab (PhytoLab GmbH & Co. KG, Vestenbergsgreuth, Germany), namely heliotrine (minimum 85% (HPLC), lycopsamine (minimum 85% (HPLC)), and senecionine (minimum 85% (HPLC)). The pyrrolizidine alkaloid reference substances were dissolved in acetonitrile in the first step. The appropriate final concentration was achieved by dilution with Milli-Q™ water. Caffeine (ReagentPlus®, minimum 99%), halloysite nanoclay, monocrotaline (≥98%), anhydrous toluene (99.8%), triethoxyphenlysilane (≥98%) and 3-(mercaptopropyl)trimethoxysilane (95%) were ordered from Sigma-Aldrich (Sigma-Aldrich, St. Louis, USA). Purified water was collected from a Merck Millipore Milli-Q™ Reference Ultrapure Water Purification System. Empty 1 mL polypropylene SPE cartridges with prefiltration (polyethylene, 20 mm porosity) were acquired from Sigma-Aldrich.

2.1.2. Honey Sample

Honey from Bergland-Honig (Bergland-Honig GmbH, Urban, Austria) was purchased from a nearby convenience store to analyze a spiked field sample. The honey was prepared as described in the following chapter, without the addition of analytes. The analyte-free real sample was analyzed for pyrrolizidine alkaloids prior to the experiments using the developed UHPLC-MS/MS method to prevent any possible bias.

2.1.3. Sample Preparation

A slightly modified method, compared to our previous study [18], was used to prepare the honey sample. For this purpose, 4 g of bee honey was completely dissolved in 40 mL of 0.05 M formic acid (FA) in a falcon tube by shaking. Centrifugation was then carried out at 14,000 rpm for 10 min. Subsequently, an aqueous standard solution of the pyrrolizidine alkaloids heliotrine, lycopsamine, monocrotaline, and senecionine was then added to the sample to get a final concentration of 12.5 µg L^{-1} per pyrrolizidine alkaloid. These pyrrolizidine alkaloids were selected because they represent four of the six main structures of this class of compounds. The spiking amount was based on the current European Union regulation for pyrrolizidine levels in honey. This states that a maximum level of 500 µg kg^{-1} of pyrrolizidine alkaloids in food supplements, pollen and pollen-based products must not be exceeded [31].

2.1.4. Synthesis of Organosilyl-Sulfonated Halloysite Nanotubes

Synthesis of both alkyl-sulfonated halloysite nanotube materials was achieved according to a similar protocol published by Silva et al. [17] and Peixoto et al. [16]. The scales of the reactions were altered if needed. In the following subsections, the general synthesis steps of both materials will be described more thoroughly. Before using both synthesized materials for solid phase extraction, grinding was performed to achieve a more uniform distribution of particles.

HNT-PhSO_3H

In the first step of the synthesis of HNT-PhSO_3H, 2 g of dry halloysite nanotubes were suspended in 100 mL anhydrous toluene and 1.5 mmol triethoxyphenylsilane (PhTES).

The mixture was then refluxed for 24 h under constant stirring and nitrogen atmosphere. Subsequently, the product HNT-PhTES was centrifuged, washed with four 10 mL portions of toluene and dried at 100 °C for 24 h.

For the chlorosulfonation in the second step, 2 g of the previously synthesized HNT-PhTES were added to 30 mL of dichloromethane. Afterwards, 2.4 mL of chlorosulfonic acid were added dropwise to the mixture, which was then refluxed at 50 °C for 6 h. The resulting HNT-PhSO_3H material was then centrifuged, washed with four 10 mL portions of methanol and dried at 100 °C for 24 h. The synthesis steps are shown in Figure 1.

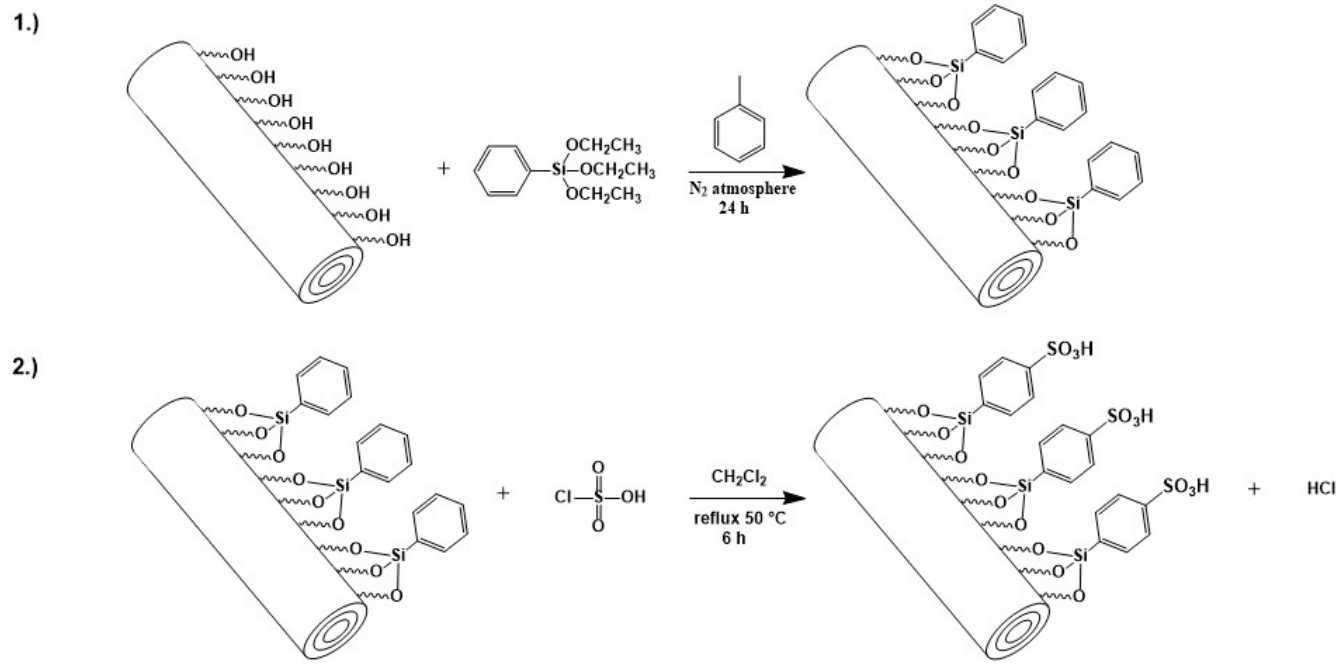

Figure 1. Two-step synthesis of HNT-PhSO_3H consisting of organosilylation (**1.**) and sulfonation step (**2.**) according to Silva et al. and Peixoto et al. [16,17].

HNT-MPTMS-SO_3H

Prior to the synthesis, 2 g of halloysite nanotubes were dried at 100 °C for 1 h. Subsequently, the organosilylation of the dried halloysite nanotubes was achieved through the dropwise addition of 1.13 mL (6 mmol) (3-mercaptopropyl)trimethoxysilane to 2 g of HNTs suspended in 100 mL anhydrous toluene. The reaction mixture was refluxed under constant stirring and nitrogen atmosphere for 24 h. This was followed by centrifugation and washing of the resulting HNT-MPTMS with four 10 mL portions of toluene and drying at 100 °C for 24 h.

In the second step of the synthesis, 2 g of HNT-MPTMS were suspended in 30 mL of dichloromethane through constant magnetic stirring while cooling the mixture with the help of an ice bath for 10 min. This was followed by the addition of 3.4 mL of chlorosulfonic acid through a constant pressure dropping funnel. The reaction mixture was then stirred for 4 h at room temperature with an equipped Dimroth condenser. The final HNT-MPTMS-SO_3H was then centrifuged, washed with four 10 mL portions of methanol and dried at 100 °C. Figure 2 shows the respective synthesis steps.

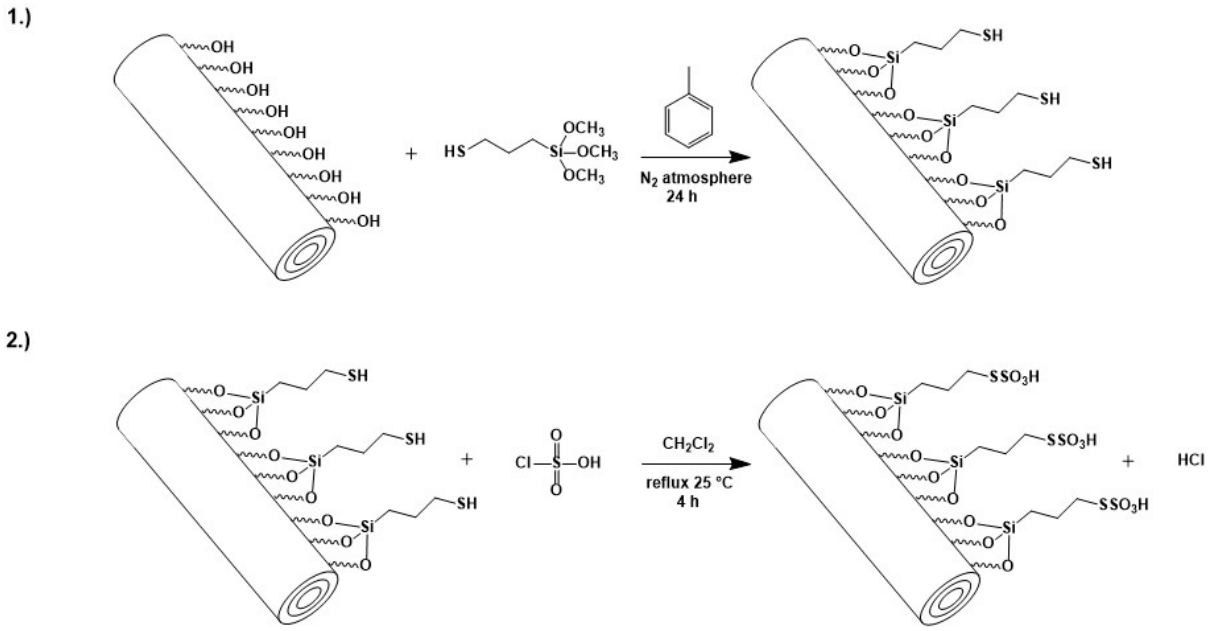

Figure 2. Two-step synthesis of HNT-MPTMS-SO_3H consisting of organosilylation (**1.**) and sulfonation step (**2.**) according to Silva et al. and Peixoto et al. [16,17].

2.1.5. FT-ATR Analysis

To verify the structural change in the modified halloysite nanotubes, FT-ATR analysis was performed with a PerkinElmer Spectrum 100 FT-IR Spectrometer (PerkinElmer Inc., Waltham, MA, USA) equipped with a universal ATR sampling accessory. Measurements were recorded in the range of 650 cm^{-1} to 4000 cm^{-1}.

2.1.6. Solid Phase Extraction

Solid phase extraction protocols were optimized using an aquatic 10 µg L^{-1} standard mixture of four pyrrolizidine alkaloids, namely heliotrine, lycopsamine, monocrotaline and senecionine as they present four of the six main structures of the pyrrolizidine alkaloid compound group. A schematic workflow starting from sample preparation up to UHPLC-MS/MS analysis can be seen in Figure 3.

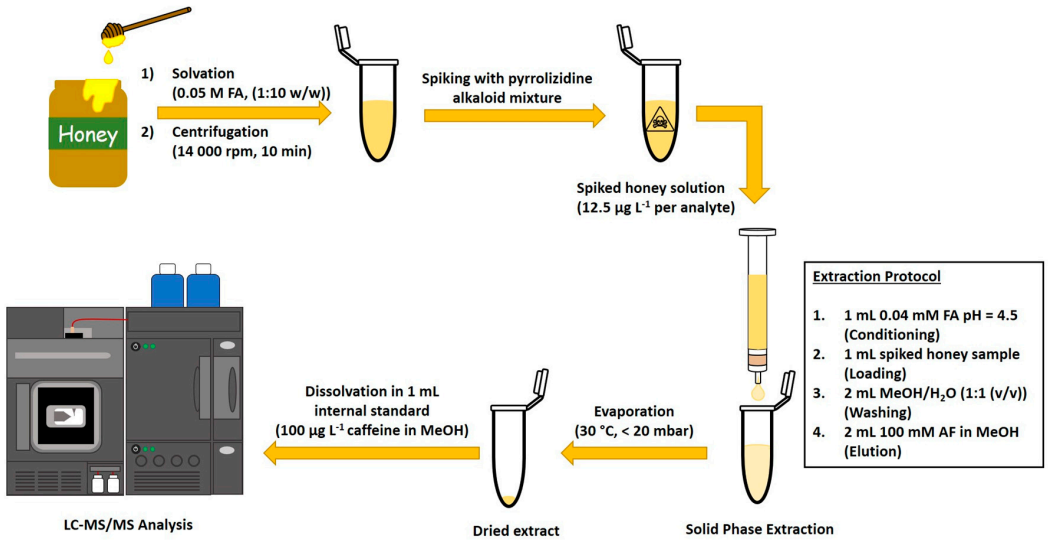

Figure 3. Schematic display of the experimental workflow using organosilyl-sulfonated halloysite nanotubes as material for solid phase extraction of toxic pyrrolizidine alkaloids in honey matrix.

Pyrrolizidine Alkaloid Standard Mixture Extraction

Empty, pre-fritted 1 mL solid phase extraction tubes were filled with 50 mg of ground organosilyl-sulfonated halloysites and covered with an additional 0.2 µm polyethylene (PE) frit. A force meter was used to press all cartridges with a weight of 2.5 kg to ensure uniform packing and reproducibility. For conditioning, 1 mL of 0.04 mM formic acid solution with a pH of 4.5 was used. Before the conditioning solvent reached the level of the first PE frit, 1 mL of aquatic pyrrolizidine alkaloid standard mixture was added onto the material. In order to decrease the pH of the sample, leading to the protonation of the nitrogen atom of the pyrrolizidine alkaloids, the standard mixture was diluted with conditioning solvent. However, since no effect was visible, this step was not implemented in the final extraction protocol. After the complete passing of the sample through the solid phase elution was performed with 2 mL of 100 mM ammonium formate in methanol. All steps were performed with the help of pressured air at a drop rate of three to four drops per minute. The residues of the sample after loading as well as the eluates of the solid phase extraction were then dried at 30 °C under vacuum and resuspended in 1 mL 100 µg L^{-1} caffeine solution in dimethylsulfoxide/methanol 1/1 (v/v).

Spiked Honey Sample

Solid phase extraction of spiked honey sample and blank honey matrix was achieved through the identical protocol, which was used for the pyrrolizidine standard mixture. Furthermore, an additional washing step consisting of two portions of methanol/water 1/1 (v/v) was implemented. This was conducted to further reduce matrix effects originating from competing substances of the honey matrix. In our last work, this was not possible due to the weaker binding of the pyrrolizidine alkaloids to the solid material [18].

- Validation

To present the effectiveness and competitiveness of the synthesized solid materials for solid phase extraction, validation was performed for HNT-MPTMS-SO_3H. All parameters were determined according to found literature [37–41] and only slightly modified.

Specificity

Specificity was ensured through the use of highly selective multi reaction monitoring mode. Furthermore, blank solvent and honey matrix were analyzed with the presented UHPLC-MS/MS method to prove high specificity.

Linearity

Linearity was determined through measurement of three independently prepared matrix match calibrations with eight concentration steps ranging from 0 µg L^{-1} to 14 µg L^{-1} (0, 16, 32, 48, 64, 80, 96 and 112% of target concentration, respectively). The sample preparation protocol and UHPLC-MS/MS method was chosen identically to the final procedure.

Bias

Bias was calculated according to the following formula [39].

$$Bias\ [\%] = \frac{\overline{x} - \mu}{\mu} \cdot 100\% \quad (1)$$

where $\overline{x}$ represents the averaged value of each concentration step and µ represents the reference value.

LOD and LOQ

Limit of detection and limit of quantification were calculated according to DIN 32645 [37], using the following formulas.

$$LOD = s_{x_0} \cdot t_{f,\alpha} \sqrt{\frac{1}{m} + \frac{1}{n} + \frac{\overline{x}^2}{Q_x}} \quad (2)$$

$$LOD = s_{x_0} \cdot t_{f,\alpha} \sqrt{\frac{1}{m} + \frac{1}{n} + \frac{((k \cdot LOD) - \overline{x})^2}{Q_x}} \quad (3)$$

Parameters in the previous two equations are s_{x_0}, which describes the procedure standard deviation of the regression curve, and t, which represents the student factor with $P = 95\%$ used one-sided for the LOD calculation and two-sided for LOQ calculation. Additionally, m is the number of replicate measurements and n displays the number of calibration points. $\overline{x}$ describes the arithmetic mean of all calibration concentrations, while Q_x describes the term $\sum_{i=1}^{n}(x_i - \overline{x})^2$. Furthermore, $k{\cdot}LOD$ was used as approximation, since the LOQ is usually calculated iteratively, for which $k = 3$ was chosen.

Loading Efficiency

Loading efficiency was determined through the measurement of ten independent residues of the extracted spiked samples after solid phase extraction in triplicate.

Recovery

Recovery was assessed by performing ten independent solid phase extractions of spiked honey sample (12.5 µg L^{-1} of each pyrrolizidine alkaloid) and comparing the measured analyte and internal standard areas with a matrix matched calibration curve. Each sample was measured in triplicate. Standard deviation of each triplicate measurement was calculated according to the formula based on the formula for random sampling of the data set.

Repeatability

Repeatability was determined from ten independent experiments at 100% of the target concentration. Experiments were executed by the same operator on the same day. Subsequently, ten solid phase extractions were independently performed with a honey sample spiked with 12.5 µg L^{-1} of each of the four pyrrolizidine alkaloids. Each eluate of the solid phase extraction was measured in triplicate. Repeatability was then calculated as RSD in % with the standard deviation formula based on random sampling of the data set.

Matrix Effect

Matrix effect was calculated through the comparison of slopes between a matrix matched calibration curve and a calibration curve of the same levels (0–14 µg L^{-1}) in pure solvent with 200 mM ammonium formate, since it is also present in this amount in the matrix extracts, according to the following formula [42].

$$ME[\%] = \frac{k_{MM}}{k_{Solvent}} \cdot 100\% \quad (4)$$

With k_{MM} representing the slope of the matrix matched calibration and $k_{Solvent}$ representing the slope of the calibration in pure solvent. Each calibration curve was measured in triplicate.

Autosampler Stability

Autosampler stability was tested through the measurement of three matrix matched calibration samples at low, medium and high concentration levels (4, 8 and 12 µg L^{-1}, respectively) in triplicate after every 6 h in a range of 48 h. Subsequently, the fraction of areas multiplied with the concentration of the internal standard were calculated for each measurement. Freshly prepared solutions (e.g., 0 h) were used as 100% to normalize the consecutive averaged triplicate measurements.

Reusability Study

As environmentally friendly and sustainable chemistry becomes more and more important in today's world, the HNT-MPTMS-SO_3H material was checked for its multiple usability. Solid phase extraction of the aqueous 10.0 µg L^{-1} pyrrolizidine standard solution was therefore performed as earlier specified. In order to cleanse the solid material for re-use and prevent carryover from preceding extractions, we conducted our previously published protocol for the reusability study [18]. As in general, the first washing step was carried out with two extra portions of 1 mL each of the methanolic 100 mM ammonium formate solution. Subsequently, the material was washed twice with 1 mL methanol each. To verify the efficiency of the washing steps, UHPLC-MS/MS analysis of the washing steps was carried out, which revealed no traces of pyrrolizidine alkaloids. Subsequently, the solid in

the cartridge was pre-dried with compressed air for 3 min before being completely dried at 50 °C for 10 min [18]. This procedure was performed before each new replicate cycle, so that a total of six SPE cycles could be performed with the same cartridge. After that, the experiments were stopped as the evidence for reusability could be clearly presented.

2.1.7. UHPLC-MS/MS Analysis

A Waters Acquity Premier liquid chromatograph with a Waters TQD triple quadrupole detector was used for UHPLC-MS/MS analysis. The sheath and auxiliary gas was nitrogen, whereas argon represented the collision gas. A Thermo Fisher Hypersil Gold™ C18 Selectivity column measuring 150 × 2.1 mm with a particle size of 1.9 mm, identical to official analysis protocols, was used [30,32]. The column oven was set to 50 °C, while the temperature of the autosampler was fixed at 25 °C. The injection volume was adjusted to 1 µL using 10% acetonitrile in water as wash solution. Analysis was performed in binary gradient mode with 0.1% FA in H_2O (A) and acetonitrile (B) at a flow rate of 0.4 mL min^{-1}, similar to our previous work [18]. The following solvent composition was applied during analysis: 0.0–1.0 min (5% B), 1.0–7.5 min (5–50% B), 7.5–7.6 min (50–100% B), 7.6–8.3 min (100% B), 8.3–8.4 min (100–5% B), and 8.4–13.0 min (5% B). Waters MassLynx was used for acquisition. Multiple reaction monitoring (MRM) method tuning and generation was performed in positive electrospray (ES) mode using Waters' IntelliStart software. The measurements were carried out using the tuning method of monocrotaline, as it is a representative of the compound class. MRM methods for each analyte were created under solvent flow with initial gradient solvent composition. Three transitions per analyte, except for the structurally smaller internal standard caffeine, were selected for quantification via their total ion chromatogram (TIC). In Table 1, the transitions of the four pyrrolizidine alkaloids and caffeine (IS) are shown with the corresponding retention times, cone and collision voltages. A measurement of a 1 mg L^{-1} thiourea solution revealed the dead time of the used method. To protect the mass spectrometer from unwanted contaminants such as highly polar substances, e.g., salts and saccharides, as well as strong nonpolar compounds, the MS acquisition was initiated after 1.5 min and stopped after 7.5 min. Data analysis was carried out using TargetLynx.

Table 1. Retention times and tandem MS parameters of the analyte transitions observed in MRM mode.

Compound	R_t/min	Precursor Ion $[M + H]^+$	Product Ions	Cone Voltage/V	Collision Voltage/V
Monocrotaline	2.0	326	94; 120; 194	58	42; 32; 34
Lycopsamine	3.3	300	94; 138; 156	50	32; 22; 28
Caffeine (IS)	4.0	195	41; 138	32	40; 18
Heliotrine	4.5	314	94; 138; 156	44	44; 22; 30
Senecionine	5.1	336	93(.5); 93(.9); 120	58	48; 34; 38

3. Results and Discussion

3.1. Synthesis of Organosilyl-Sulfonated Halloysite Nanotubes

MIR-ATR Analysis

FT-ATR analyses of both synthesized, modified halloysite nanotubes showed newly appearing signals in the spectrum compared to the unmodified halloysite nanoclay. These are in accordance with the results obtained by Silva et al. [17].

3.2. Solid Phase Extraction

3.2.1. SPE with Unmodified Halloysite Nanotubes

To verify that modification of halloysite nanotubes is necessary to improve their properties as cation-exchange material for solid phase extraction, unmodified halloysite nanoclay was tested. Therefore, raw, unmodified halloysite nanotubes were used as solid phase extraction material for the extraction of an aqueous 10 µg L^{-1} pyrrolizidine alkaloid mixture. Furthermore, the same procedure used for the modified materials was

performed. However, solid phase extractions could not be executed as the backpressure of the unmodified material was too high to pass the solvent through the packed cartridge in a practical manner. As a result of this, structural modification of the raw halloysite nanotubes is necessary to perform solid phase extractions at a reasonable backpressure to ensure a well-working sample preparation method. These results are identical to the solid phase extractions of unmodified halloysite nanotubes from our last work [18].

3.2.2. Pyrrolizidine Alkaloid Standard Mixture

HNT-$PhSO_3H$

To validate the performance of the synthesized modified halloysite nanotubes, solid phase extractions were performed with an aqueous 10.0 µg L^{-1} pyrrolizidine alkaloid mixture, according to the previously described extraction protocol. Table 2 shows the averaged recoveries of the four pyrrolizidine alkaloids after performing solid phase extraction using HNT-$PhSO_3H$. Hence, high recoveries of at least 81.5% for monocrotaline and up to 99.8% for heliotrine could be observed. Batch to batch recoveries are displayed in Figure 4. Subsequently, an analysis of the breakthrough showed only noise which displays high loading efficiency of the pyrrolizidine alkaloids on the solid material.

Table 2. Recoveries of an aqueous 10.0 µg L^{-1} pyrrolizidine alkaloid standard mixture after solid phase extraction using HNT-$PhSO_3H$ and HNT-MPTMS-SO_3H as solid materials.

Recovery ± SD /% (N = 10; HNT-$PhSO_3H$)			
Monocrotaline	**Lycopsamine**	**Heliotrine**	**Senecionine**
81.5 ± 3.4	98.3 ± 7.3	99.8 ± 5.1	92.1 ± 6.8
Recovery ± SD/% (N = 10; HNT-MPTMS-SO_3H)			
Monocrotaline	Lycopsamine	Heliotrine	Senecionine
78.3 ± 5.8	101.3 ± 5.9	99.1 ± 2.6	81.3 ± 5.7

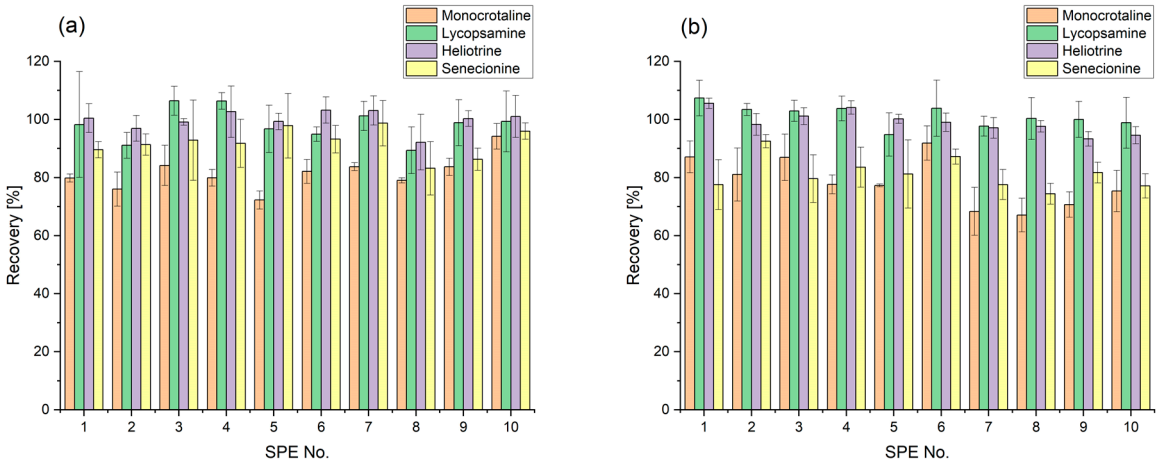

Figure 4. Solid phase extraction of an aqueous 10.0 µg L^{-1} pyrrolizidine alkaloid standard mixture using HNT-$PhSO_3H$ (**a**) and HNT-MPTMS-SO_3H (**b**) as solid phase.

HNT-MPTMS-SO_3H

The second modified organosilyl-sulfonated halloysite nanotubes were also investigated for their extraction performance using an aqueous 10.0 µg L^{-1} pyrrolizidine alkaloid mixture. Control measurements of the breakthrough have shown to be identical to the previously described HNT-$PHSO_3H$ material, as only noise could be observed in the UHPLC-MS/MS analysis. Similar recoveries compared to HNT-$PhSO_3H$ could be achieved. The highest average recovery was obtained for lycopsamine with 101.3% and the lowest recovery for monocrotaline with 78.3%, as visible in Table 2. Batch to batch recoveries for ten performed solid phase extractions and a direct comparison to the previously presented material are displayed in Figure 4.

3.2.3. Spiked Honey Sample

As both synthesized materials, HNT-PhSO_3H and HNT-MPTMS-SO_3H, revealed satisfying performance during the solid phase extraction of the aqueous 10.0 µg L^{-1} pyrrolizidine alkaloid standard, further extractions of spiked honey samples, with the adjusted pyrrolizidine alkaloid limit for honey were conducted.

HNT-PhSO_3H

Solid phase extraction for the spiked honey sample was executed as described earlier. Therefore, the same extraction protocol was performed for the aqueous pyrrolizidine alkaloid mixture, with additional washing steps implemented. Table 3 includes the obtained averaged recoveries and matrix effects for solid phase extractions with HNT-PhSO_3H as solid material. When comparing these results with the extractions of the aqueous sample mixture, an obvious decrease in recovery for all analytes is visible. Senecionine and heliotrine still show acceptable values, however, monocrotaline and lycopsamine could not be sufficiently recovered, as visible in Figure 5. After solid phase extraction, the breakthrough partly showed large residues of these compounds. Structural properties such as the phenyl group supporting van der Waals and π-π interactions with interfering compounds from the honey matrix could be a pillar of this hypothesis. However, the reduction in the matrix effect could be achieved to a large extent, as the strongest matrix effect was obtained for lycopsamine with only +1.8%.

Table 3. Recoveries and matrix effect of a 12.5 µg L^{-1} spiked honey sample after solid phase extraction with HNT-PhSO_3H as solid material.

Recovery ± SD/% (N = 10)			
Monocrotaline	**Lycopsamine**	**Heliotrine**	**Senecionine**
62.5 ± 4.4	35.8 ± 2.0	75.9 ± 3.2	86.8 ± 8.0
Matrix Effect/%			
Monocrotaline	Lycopsamine	Heliotrine	Senecionine
98.3	101.8	100.1	93.3

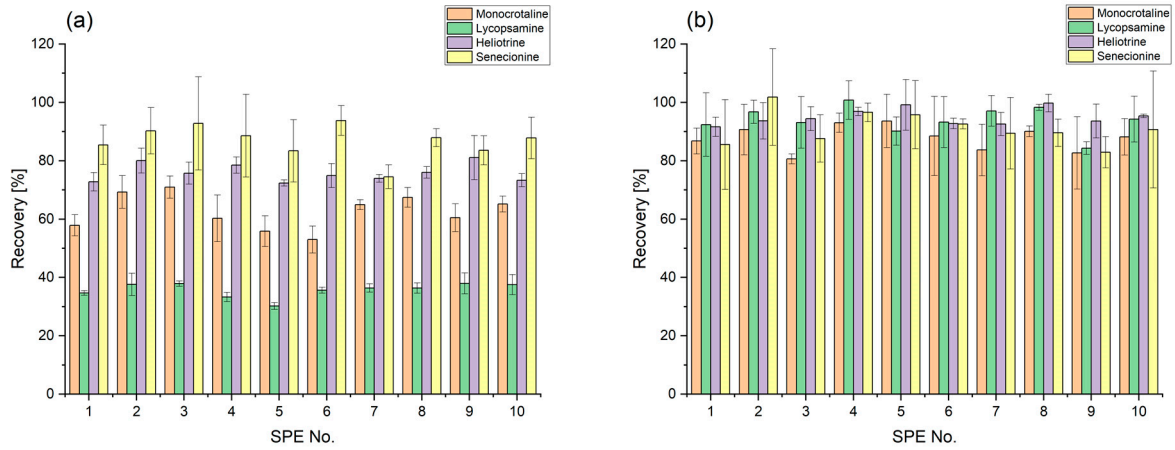

Figure 5. Solid phase extractions of a 12.5 µg L^{-1} spiked honey sample with HNT-PhSO_3H (**a**) and HNT-MPTMS-SO_3H (**b**) as solid phase.

HNT-MPTMS-SO_3H

When comparing analyte recoveries in the eluate using HNT-MPTMS-SO_3H with the previously described recoveries of HNT-PhSO_3H (Figure 5) as solid, it becomes apparent that significantly higher recoveries can be achieved by using HNT-MPTMS-SO_3H. Average values present high recoveries up to 95.0% for heliotrine when using HNT-MPTMS-SO_3H. In comparison, HNT-PhSO_3H as solid material reveals recoveries of up to 86.8% for senecionine, while lycopsamine shows only poor recoveries of 35.8%. For this reason, validation was only performed for HNT-MPTMS-SO_3H.

- Validation

Specificity

Pyrrolizidine alkaloids were detected in highly specific multiple reaction monitoring mode. Hence, the combination of nominal precursor and product ions have to be given to fulfil detection criteria. Therefore, high specificity should be given theoretically. However, measurements of blank solvents and blank matrix were executed with the previously presented UHPLC-MS/MS method, which revealed no observable pyrrolizidine alkaloid signals.

Linearity

Coefficients of determination show satisfying R^2 values up to 0.992 and therefore display good linearity of the method. The calibration curves of the selected four analytes can be found in the supplementary information (Figure S1).

Bias

Bias values were calculated according to Equation (1). Table 4 shows the bias values of a low-, medium- and high-concentrated matrix-matched calibration solution. The obtained values are within the limit of ±15% and can therefore be seen as acceptable [39].

Table 4. Validation parameters of the presented method using HNT-MPTMS-SO_3H and 12.5 µg L^{-1} spiked honey sample.

Bias/%				
Concentration level/µg L^{-1}	Monocrotaline	Lycopsamine	Heliotrine	Senecionine
4	±5.95	±2.07	±1.36	±10.0
8	±11.3	±2.47	±7.36	±2.85
12	±5.07	±0.03(4)	±3.67	±1.89
Limit of detection and Limit of quantification/µg L^{-1}				
	Monocrotaline	Lycopsamine	Heliotrine	Senecionine
LOD	1.0	0.7	0.6	1.2
LOQ	3.2	2.3	1.9	3.6
Recovery ± SD/% (N = 10)				
Monocrotaline		Lycopsamine	Heliotrine	Senecionine
87.8 ± 7.0		94.0 ± 6.0	95.0 ± 3.9	91.3 ± 9.9
Repeatability RSD/% (N = 10)				
Monocrotaline		Lycopsamine	Heliotrine	Senecionine
5.0		4.9	2.9	6.2
Matrix Effect/%				
Monocrotaline		Lycopsamine	Heliotrine	Senecionine
106.6		104.1	110.1	102.2

LOD and LOQ

In Table 4, the respective limits of detection and quantification, calculated according to DIN 32645 [37] Equations (2) and (3), are displayed, respectively. The limit of detection values for lycopsamine and heliotrine are in the ng L^{-1} range, whereas monocrotaline and senecionine show values in the low µg L^{-1} area. Therefore, both parameters demonstrate the suitability of the presented method for highly precise analysis of pyrrolizidine alkaloids in honey matrix.

Loading Efficiency

Measurements of the breakthrough from spiked honey samples showed only noise for all analytes at the respective retention times after solid phase extraction with HNT-MPTMS-SO_3H. Therefore, pyrrolizidine alkaloid levels can only be smaller than the respective limits of detection from Table 4. Hence, the loading step of the sample onto HNT-MPTMS-SO_3H for solid phase extraction can be seen as highly efficient and selective as complete adsorption of the compounds of interest takes place in a complex matrix such as honey.

Recovery

Table 4 shows the obtained averaged recoveries of all target analytes in the eluate from ten performed solid phase extractions. When comparing these results with the extraction of the aqueous pyrrolizidine alkaloid mixture, which was presented in a previous section, averaged recovery values for monocrotaline and senecionine present slightly better results, whereas lycopsamine and heliotrine show a small decrease. However, when standard deviation is included, the recovery ranges overlap. Therefore, no decrease in recovery is visible when performing solid phase extractions with a highly complex matrix such as honey. Looking at publications that use solid phase extractions as sample preparation for pyrrolizidine alkaloid analysis (Table 5), it can be seen that the recoveries of the method presented here are competitive [43–47].

Table 5. Recovery rates of pyrrolizidine alkaloids in different matrix in previously published solid phase extraction methods.

Sample Matrix	Recovery Range/%	Solid Phase Material	Literature
Gynura procumbens	21.8–99.4	PCX	[43]
Gynura procumbens	21.6–96.1	SCX	[43]
Gynura procumbens	57.8–101.9	C18	[43]
Gastrodia elata	77.6–101.4 *	MCX	[44]
Atractylodes japonica	85.2–101.9 *	MCX	[44]
Leonurus japonicus	93.3–112.7 *	MCX	[44]
Glycyrrhiza uralensis	73.8–98.1 *	MCX	[44]
Chrysanthemum morifolium	70.6–103.5 *	MCX	[44]
Tussilago farfara	73.1–111.4 *	MCX	[45]
Lithospermi erythrorhzion	72.3–118.3 *	MCX	[45]
Tussilago farfara	92.5–103.5	MIP	[46]
Herbal teas (fennel, mixed tea and rooibos)	72–122	C18	[47]
Honey (cornflower and lavender)	66–96	C18	[47]

* recoveries from medium spike levels.

Furthermore, the presented method also competes with sample preparation methods other than solid phase extraction in terms of analyte recovery, as the values already reported here are within the recovery ranges of the published methods [42,48–50].

Repeatability

Residual standard deviation values describing the repeatability of the presented method are displayed in Table 4. RSD values ranging from 2.9% up to 6.2% could be obtained. This can be seen as acceptable results, since cartridges were self-packed and therefore variation in packing is inevitable.

Matrix Effect

Matrix effects for all analyzed compounds of interest, which were calculated according to Equation (4), are displayed in Table 4. Values ranging from 102.2% to 110.1% could be obtained, showing slight ion enhancement for each compound of interest. According to the literature, the matrix effect of this method can be classified as soft [51,52]. Hence, matrix-matched calibration would not be necessary for the newly presented method, as matrix effects can be sufficiently reduced [42]. Furthermore, the novel method shows a significantly better reduction in matrix effects than in our last work, where we observed medium matrix effects for most analyzed compounds [18]. This can be reasoned due to the additional washing step, which is now possible due to the stronger binding of the analytes onto the solid material.

Autosampler Stability

Figure 6 displays the averaged triplicate measurements of each concentration level every six hours. The stability of the low concentrated matrix-matched standard, close to the limit of quantification, showed no deviations higher than 20%, with the exception of the 6 h measurement of senecionine (±79.8%) [39]. However, stability values of this sample

before and after these durations suggest a random instrument error for this triplicate measurement, as they present in-range values. Subsequently, no deviations more than ±15% were observed for the medium and high concentration levels (8 and 12 µg L^{-1}) [39]. Therefore, acceptable stability of the samples in the autosampler is given.

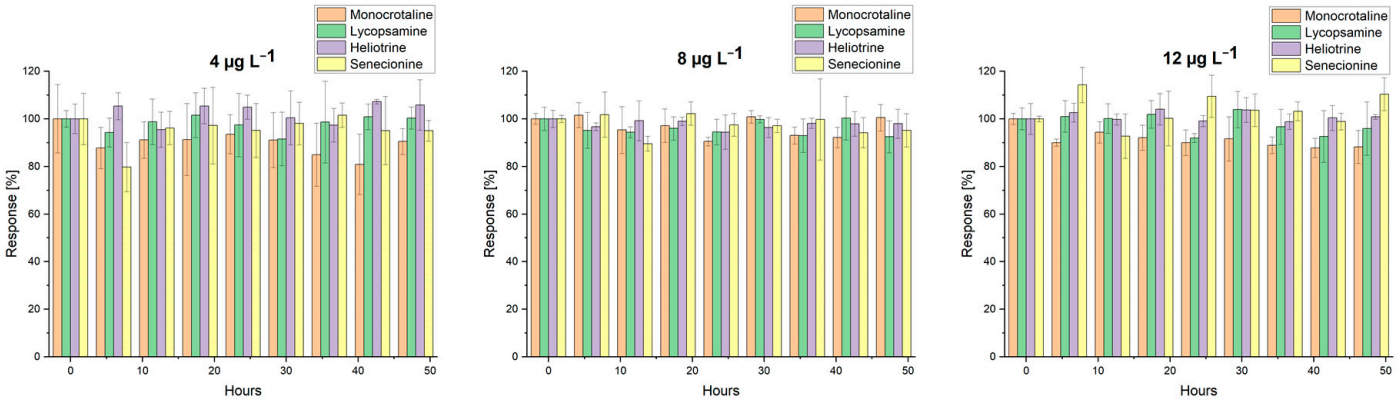

Figure 6. Autosampler stability of matrix-matched calibration standards with low, medium and high concentrations of pyrrolizidine alkaloids.

3.2.4. Reusability Study

Figure 7 displays the recoveries of all four compounds of interest after six SPE cycles, performed according to the previously described reusability protocol. Hence, the HNT-MPTMS-SO_3H material can be reused multiple times, as no significant decrease in recovery can be observed when taking the error bars into account. Subsequently, Table 6 displays the recovery consistency over all six performed solid phase extraction cycles with no signs of loss in performance or destruction of the solid material. After six SPE cycles, the test was terminated, since the reusability could be fully demonstrated. However, since no deficits in recovery rates or phase stability are apparent, use over six cycles is highly likely.

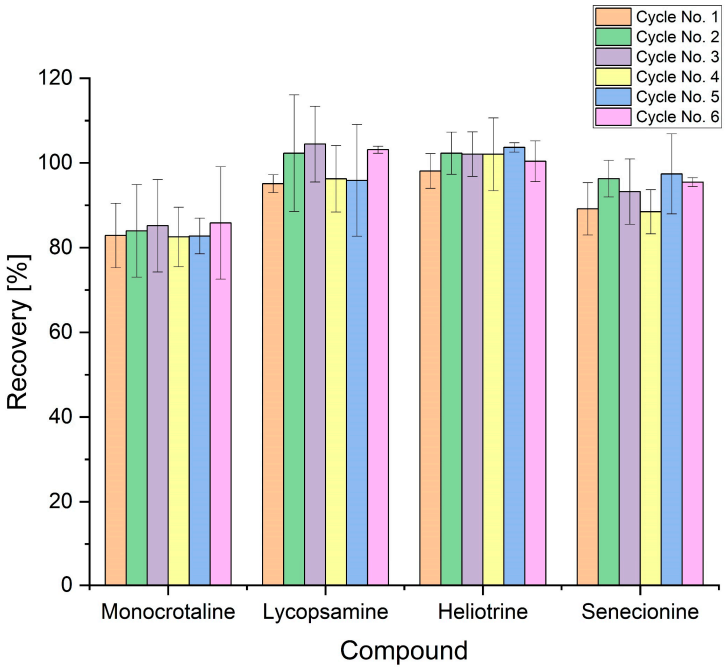

Figure 7. Recoveries of an aqueous 10.0 µg L^{-1} pyrrolizidine alkaloid mixture after six consecutive solid phase extractions with HNT-MPTMS-SO_3H.

Table 6. Averaged recoveries over six cycles of solid phase extraction using the same HNT-MPTMS-SO_3H solid material.

SPE Cycle No.	Recovery ± SD/%			
	Monocrotaline	**Lycopsamine**	**Heliotrine**	**Senecionine**
1	82.9 ± 7.6	95.1 ± 2.0	98.1 ± 4.1	89.2 ± 6.2
2	84.0 ± 10.9	102.3 ± 13.8	102.3 ± 5.0	96.3 ± 4.3
3	85.2 ± 10.9	104.5 ± 8.9	102.1 ± 5.3	93.2 ± 7.7
4	82.5 ± 7.0	96.3 ± 7.8	102.0 ± 8.6	88.5 ± 5.2
5	82.7 ± 4.2	95.9 ± 13.2	103.7 ± 1.1	97.4 ± 9.5
6	85.8 ± 13.3	103.1 ± 0.8	100.4 ± 4.8	95.5 ± 1.1

4. Conclusions

Two modified halloysite nanotubes were tested for their performance in the selective solid phase extraction of toxic pyrrolizidine alkaloids as alternative candidates to polymeric resins. Both materials showed satisfying results in the extraction of an aqueous pyrrolizidine alkaloid mixture containing four of the six main structures of the pyrrolizidine alkaloid group. In addition, solid phase extraction of spiked honey samples was performed with both materials considering the respective maximum pyrrolizidine alkaloid level. While the HNT-PhSO_3H material showed a significant decrease for some analytes, yet good matrix reduction properties, the use of the HNT-MPTMS-SO_3H material does not lead to a decrease in recoveries when compared to the aqueous analyte mixture. Therefore, the latter was validated and displayed acceptable results. Matrix effects could be reduced down to a maximum of 10.1% when compared to our last work. In addition, repeatability presents satisfying values for self-packed solid phase tubes. To make a further step towards green chemistry, the solid material was tested for reusability and showed excellent performance over six solid phase extraction cycles with no decrease in recovery or depletion of the solid material. Comparing the recoveries obtained with the results of solid phase extractions using commercial SCX cartridges performed in our last work with the same pyrrolizidine alkaloids, concentrations and matrix, the significantly better performance of the mercaptopropyl-sulfonated halloysite material is again evident. Furthermore, halloysite nanotubes can once again be presented as an economical and environmentally friendly resource due to their massive natural occurrence and resulting low cost. Hence, a green, sustainable and novel solid material for selective solid phase extraction of toxic pyrrolizidine alkaloids from honey can be presented to further develop additional environmentally friendlier alternatives compared to usual used polymeric substrates in solid phase extraction.

Supplementary Materials: The following supporting information can be downloaded at: https://www.mdpi.com/article/10.3390/separations9100270/s1, Figure S1: Calibration curves of the four analytes, namely monocrotaline, lycopsamine, heliotrine and senecionine.

Author Contributions: Conceptualization, T.S. and M.R.; data curation, T.S. and N.W.; formal analysis, T.S. and N.W.; investigation, T.S. and N.W.; methodology, T.S. and N.W.; project administration, M.R.; supervision, M.R.; validation, T.S. and N.W.; visualization, T.S.; writing—original draft, T.S.; writing—review & editing, C.W.H., G.K.B. and M.R. All authors have read and agreed to the published version of the manuscript.

Funding: This research received no funding.

Conflicts of Interest: There are no conflict to declare.

References

1. Lazzara, G.; Cavallaro, G.; Panchal, A.; Fakhrullin, R.; Stavitskaya, A.; Vinokurov, V.; Lvov, Y. An Assembly of Organic-Inorganic Composites Using Halloysite Clay Nanotubes. *Curr. Opin. Colloid Interface Sci.* **2018**, *35*, 42–50. [CrossRef]
2. Yuan, P.; Tan, D.; Annabi-Bergaya, F. Properties and Applications of Halloysite Nanotubes: Recent Research Advances and Future Prospects. *Appl. Clay Sci.* **2015**, *112–113*, 75–93. [CrossRef]

3. Lvov, Y.; Wang, W.; Zhang, L.; Fakhrullin, R. Halloysite Clay Nanotubes for Loading and Sustained Release of Functional Compounds. *Adv. Mater.* **2016**, *28*, 1227–1250. [CrossRef]
4. El-Sheikhy, R. Exploring of New Natural Saudi Nanoparticles: Investigation and Characterization. *Sci. Rep.* **2020**, *10*, 21557. [CrossRef]
5. Nicholson, J.; Weisman, J.; Boyer, C.; Wilson, C.; Mills, D. Dry Sintered Metal Coating of Halloysite Nanotubes. *Appl. Sci.* **2016**, *6*, 265. [CrossRef]
6. Riahi-Madvaar, R.; Taher, M.A.; Fazelirad, H. Synthesis and Characterization of Magnetic Halloysite-Iron Oxide Nanocomposite and Its Application for Naphthol Green B Removal. *Appl. Clay Sci.* **2017**, *137*, 101–106. [CrossRef]
7. Vergaro, V.; Abdullayev, E.; Lvov, Y.M.; Zeitoun, A.; Cingolani, R.; Rinaldi, R.; Leporatti, S. Cytocompatibility and Uptake of Halloysite Clay Nanotubes. *Biomacromolecules* **2010**, *11*, 820–826. [CrossRef]
8. Almasri, D.A.; Saleh, N.B.; Atieh, M.A.; McKay, G.; Ahzi, S. Adsorption of Phosphate on Iron Oxide Doped Halloysite Nanotubes. *Sci. Rep.* **2019**, *9*, 3232. [CrossRef]
9. Chen, X.-G.; Li, R.-C.; Zhang, A.-B.; Lyu, S.-S.; Liu, S.-T.; Yan, K.-K.; Duan, W.; Ye, Y. Preparation of Hollow Iron/Halloysite Nanocomposites with Enhanced Electromagnetic Performances. *R. Soc. Open Sci.* **2018**, *5*, 171657. [CrossRef]
10. Joo, Y.; Sim, J.H.; Jeon, Y.; Lee, S.U.; Sohn, D. Opening and Blocking the Inner-Pores of Halloysite. *Chem. Commun.* **2013**, *49*, 4519. [CrossRef]
11. White, R.D.; Bavykin, D.V.; Walsh, F.C. The Stability of Halloysite Nanotubes in Acidic and Alkaline Aqueous Suspensions. *Nanotechnology* **2012**, *23*, 065705. [CrossRef]
12. Fizir, M.; Dramou, P.; Dahiru, N.S.; Ruya, W.; Huang, T.; He, H. Halloysite Nanotubes in Analytical Sciences and in Drug Delivery: A Review. *Microchim. Acta* **2018**, *185*, 389. [CrossRef]
13. Rawtani, D.; Pandey, G.; Tharmavaram, M.; Pathak, P.; Akkireddy, S.; Agrawal, Y.K. Development of a Novel 'Nanocarrier' System Based on Halloysite Nanotubes to Overcome the Complexation of Ciprofloxacin with Iron: An in Vitro Approach. *Appl. Clay Sci.* **2017**, *150*, 293–302. [CrossRef]
14. Tabani, H.; Khodaei, K.; Moghaddam, A.Z.; Alexovič, M.; Movahed, S.K.; Zare, F.D.; Dabiri, M. Introduction of Graphene-Periodic Mesoporous Silica as a New Sorbent for Removal: Experiment and Simulation. *Res. Chem. Intermed.* **2019**, *45*, 1795–1813. [CrossRef]
15. Moghaddam, A.Z.; Bameri, A.E.; Ganjali, M.R.; Alexovič, M.; Jazi, M.E.; Tabani, H. A Low-Voltage Electro-Membrane Extraction for Quantification of Imatinib and Sunitinib in Biological Fluids. *Bioanalysis* **2021**, *13*, 1401–1413. [CrossRef]
16. Peixoto, A.F.; Fernandes, A.C.; Pereira, C.; Pires, J.; Freire, C. Physicochemical Characterization of Organosilylated Halloysite Clay Nanotubes. *Microporous Mesoporous Mater.* **2016**, *219*, 145–154. [CrossRef]
17. Silva, S.M.; Peixoto, A.F.; Freire, C. HSO3-Functionalized Halloysite Nanotubes: New Acid Catalysts for Esterification of Free Fatty Acid Mixture as Hybrid Feedstock Model for Biodiesel Production. *Appl. Catal. A Gen.* **2018**, *568*, 221–230. [CrossRef]
18. Schlappack, T.; Rainer, M.; Weinberger, N.; Bonn, G.K. Sulfonated Halloysite Nanotubes as a Novel Cation Exchange Material for Solid Phase Extraction of Toxic Pyrrolizidine Alkaloids. *Anal. Methods* **2022**, *14*, 2689–2697. [CrossRef]
19. *Fragen und Antworten zu Pyrrolizidinalkaloiden in Lebensmitteln*; Bundesinstitut für Risikobewertung: Berlin, Germany, 2020; Volume 15, pp. 1–7.
20. *Analytik und Toxizität von Pyrrolizidinalkaloiden Sowie Eine Einschätzung des Gesundheitlichen Risikos Durch Deren Vorkommen in Honig—Stellungnahme Nr. 038/2011 des BfR vom 11 August 2011, Ergänzt am 21 Januar 2013*; Bundesinstitut für Risikobewertung: Berlin, Germany, 2013; pp. 1–37.
21. Crews, C.; Berthiller, F.; Krska, R. Update on Analytical Methods for Toxic Pyrrolizidine Alkaloids. *Anal. Bioanal. Chem.* **2010**, *396*, 327–338. [CrossRef]
22. Ma, C.; Liu, Y.; Zhu, L.; Ji, H.; Song, X.; Guo, H.; Yi, T. Determination and Regulation of Hepatotoxic Pyrrolizidine Alkaloids in Food: A Critical Review of Recent Research. *Food Chem. Toxicol.* **2018**, *119*, 50–60. [CrossRef]
23. Schrenk, D.; Gao, L.; Lin, G.; Mahony, C.; Mulder, P.P.J.; Peijnenburg, A.; Pfuhler, S.; Rietjens, I.M.C.M.; Rutz, L.; Steinhoff, B.; et al. Pyrrolizidine Alkaloids in Food and Phytomedicine: Occurrence, Exposure, Toxicity, Mechanisms, and Risk Assessment—A Review. *Food Chem. Toxicol.* **2020**, *136*, 111107. [CrossRef]
24. Wiedenfeld, H.; Edgar, J. Toxicity of Pyrrolizidine Alkaloids to Humans and Ruminants. *Phytochem. Rev.* **2011**, *10*, 137–151. [CrossRef]
25. Brugnerotto, P.; Seraglio, S.K.T.; Schulz, M.; Gonzaga, L.V.; Fett, R.; Costa, A.C.O. Pyrrolizidine Alkaloids and Beehive Products: A Review. *Food Chem.* **2021**, *342*, 128384. [CrossRef]
26. *Pyrrolizidinalkaloide in Kräutertees und Tees—Stellungnahme 018/2013 des BfR vom 5 Juli 2013*; Bundesinstitut für Risikobewertung: Berlin, Germany, 2013; pp. 1–31.
27. Casado, N.; Morante-Zarcero, S.; Sierra, I. The Concerning Food Safety Issue of Pyrrolizidine Alkaloids: An Overview. *Trends Food Sci. Technol.* **2022**, *120*, 123–139. [CrossRef]
28. PAK und Pyrrolizidinalkaloide in Getrockneten Kräutern und Gewürzen., Bundesministerium für Arbeit, Soziales, Gesundheit und Konsumentenschutz & Österreichische Agentur für Gesundheit und Ernährungssicherheit GmbH, Vienna, Austria. 2019, pp. 1–4. Available online: www.ages.at (accessed on 12 September 2022).
29. Wiedenfeld, H. Plants Containing Pyrrolizidine Alkaloids: Toxicity and Problems. *Food Addit. Contam. Part A* **2011**, *28*, 282–292. [CrossRef]

30. *Bestimmung von Pyrrolizidinalkaloiden (PA) in Honig Mittels SPE-LC-MS/MS: Methodenbeschreibung*; Bundesinstitut für Risikobewertung: Berlin, Germany, 2013; Volume 1.0, pp. 1–17.
31. European Commission. *COMMISSION REGULATION (EU) 2020/2040 of 11 December 2020 Amending Regulation (EC) No 1881/2006 as Regards Maximum Levels of Pyrrolizidine Alkaloids in Certain Foodstuffs*; Official Journal of the European Union; 2022; p. 5. Available online: eur-lex.europa.eu (accessed on 12 September 2022).
32. *Bestimmung von Pyrrolizidinalkaloiden (PA) in Pflanzenmaterial Mittels SPE-LC-MS/MS: Methodenbeschreibung*; Bundesinstitut für Risikobewertung: Berlin, Germany, 2014; Volume 2.0, pp. 1–17.
33. Chung, S.W.C.; Lam, C.-H. Development of an Analytical Method for Analyzing Pyrrolizidine Alkaloids in Different Groups of Food by UPLC-MS/MS. *J. Agric. Food Chem.* **2018**, *66*, 3009–3018. [CrossRef]
34. Griffin, C.T.; Danaher, M.; Elliott, C.T.; Glenn Kennedy, D.; Furey, A. Detection of Pyrrolizidine Alkaloids in Commercial Honey Using Liquid Chromatography–Ion Trap Mass Spectrometry. *Food Chem.* **2013**, *136*, 1577–1583. [CrossRef]
35. He, Y.; Zhu, L.; Ma, J.; Wong, L.; Zhao, Z.; Ye, Y.; Fu, P.P.; Lin, G. Comprehensive Investigation and Risk Study on Pyrrolizidine Alkaloid Contamination in Chinese Retail Honey. *Environ. Pollut.* **2020**, *267*, 115542. [CrossRef]
36. Kowalczyk, E.; Sieradzki, Z.; Kwiatek, K. Determination of Pyrrolizidine Alkaloids in Honey with Sensitive Gas Chromatography-Mass Spectrometry Method. *Food Anal. Methods* **2018**, *11*, 1345–1355. [CrossRef]
37. *DIN 32645*; Deutsches Institut für Normierung e.V. Beuth Verlag GmbH: Berlin, Germany, 2008.
38. Nasiri, A.; Jahani, R.; Mokhtari, S.; Yazdanpanah, H.; Daraei, B.; Faizi, M.; Kobarfard, F. Overview, Consequences, and Strategies for Overcoming Matrix Effects in LC-MS Analysis: A Critical Review. *Analyst* **2021**, *146*, 6049–6063. [CrossRef]
39. Peters, F.T.; Hartung, M.; Herbold, M.; Schmitt, G.; Daldrup, T. Anforderungen an Die Validierung von Analysenmethoden. *Toxichem Krimtech* **2009**, *76*, 185.
40. Shabir Ghulam, A. Step-by-Step Analytical Methods Validation and Protocol in the Quality System Compliance Industry. *J. Valid. Technol.* **2005**, *10*, 314–325.
41. Shabir Ghulam, A. A Practical Approach to Validation of HPLC Methods under Current Good Manufacturing Practices. *J. Valid. Technol.* **2004**, *10*, 210–218.
42. Izcara, S.; Casado, N.; Morante-Zarcero, S.; Pérez-Quintanilla, D.; Sierra, I. Miniaturized and Modified QuEChERS Method with Mesostructured Silica as Clean-up Sorbent for Pyrrolizidine Alkaloids Determination in Aromatic Herbs. *Food Chem.* **2022**, *380*, 132189. [CrossRef]
43. Ji, Y.-B.; Wang, Y.-S.; Fu, T.-T.; Ma, S.-Q.; Qi, Y.-D.; Si, J.-Y.; Sun, D.-A.; Liao, Y.-H. Quantitative Analysis of Pyrrolizidine Alkaloids in *Gynura Procumbens* by Liquid Chromatography–Tandem Quadrupole Mass Spectrometry after Enrichment by PCX Solid-Phase Extraction. *Int. J. Environ. Anal. Chem.* **2019**, *99*, 1090–1102. [CrossRef]
44. Jeong, S.H.; Choi, E.Y.; Kim, J.; Lee, C.; Kang, J.; Cho, S.; Ko, K.Y. LC-ESI-MS/MS Simultaneous Analysis Method Coupled with Cation-Exchange Solid-Phase Extraction for Determination of Pyrrolizidine Alkaloids on Five Kinds of Herbal Medicines. *J. AOAC Int.* **2021**, *104*, 1514–1525. [CrossRef]
45. Ko, K.Y.; Jeong, S.H.; Choi, E.Y.; Lee, K.; Hong, Y.; Kang, I.H.; Cho, S.; Lee, C. A LC–ESI–MS/MS Analysis Procedure Coupled with Solid Phase Extraction and MeOH Extraction Method for Determination of Pyrrolizidine Alkaloids in Tussilago Farfara and Lithospermi Erythrorhzion. *Appl. Biol. Chem.* **2021**, *64*, 53. [CrossRef]
46. Luo, Z.; Chen, G.; Li, X.; Wang, L.; Shu, H.; Cui, X.; Chang, C.; Zeng, A.; Fu, Q. Molecularly Imprinted Polymer Solid-phase Microextraction Coupled with Ultra High Performance Liquid Chromatography and Tandem Mass Spectrometry for Rapid Analysis of Pyrrolizidine Alkaloids in Herbal Medicine. *J. Sep. Sci.* **2019**, *42*, 3352–3362. [CrossRef]
47. Bodi, D.; Ronczka, S.; Gottschalk, C.; Behr, N.; Skibba, A.; Wagner, M.; Lahrssen-Wiederholt, M.; Preiss-Weigert, A.; These, A. Determination of Pyrrolizidine Alkaloids in Tea, Herbal Drugs and Honey. *Food Addit. Contam. Part A* **2014**, *31*, 1886–1895. [CrossRef]
48. Rizzo, S.; Celano, R.; Campone, L.; Rastrelli, L.; Piccinelli, A.L. Salting-out Assisted Liquid-Liquid Extraction for the Rapid and Simple Simultaneous Analysis of Pyrrolizidine Alkaloids and Related N-Oxides in Honey and Pollen. *J. Food Compos. Anal.* **2022**, *108*, 104457. [CrossRef]
49. Celano, R.; Piccinelli, A.L.; Campone, L.; Russo, M.; Rastrelli, L. Determination of Selected Pyrrolizidine Alkaloids in Honey by Dispersive Liquid–Liquid Microextraction and Ultrahigh-Performance Liquid Chromatography–Tandem Mass Spectrometry. *J. Agric. Food Chem.* **2019**, *67*, 8689–8699. [CrossRef]
50. Martinello, M.; Borin, A.; Stella, R.; Bovo, D.; Biancotto, G.; Gallina, A.; Mutinelli, F. Development and Validation of a QuEChERS Method Coupled to Liquid Chromatography and High Resolution Mass Spectrometry to Determine Pyrrolizidine and Tropane Alkaloids in Honey. *Food Chem.* **2017**, *234*, 295–302. [CrossRef]
51. Ferrer Amate, C.; Unterluggauer, H.; Fischer, R.J.; Fernández-Alba, A.R.; Masselter, S. Development and Validation of a LC–MS/MS Method for the Simultaneous Determination of Aflatoxins, Dyes and Pesticides in Spices. *Anal. Bioanal. Chem* **2010**, *397*, 93–107. [CrossRef]
52. Kaczyński, P.; Łozowicka, B. A Novel Approach for Fast and Simple Determination Pyrrolizidine Alkaloids in Herbs by Ultrasound-Assisted Dispersive Solid Phase Extraction Method Coupled to Liquid Chromatography–Tandem Mass Spectrometry. *J. Pharm. Biomed. Anal.* **2020**, *187*, 113351. [CrossRef]